Epitaxial Phase Stability of SrMnO$_{3-x}$ Films on Polycrystalline Perovskite Substrates

Catherine Zhou, Gregory S. Rohrer, Marc De Graef, and Paul A. Salvador*

Read Online

ACCESS | Metrics & More | Article Recommendations

ABSTRACT: Combinatorial substrate epitaxy (CSE) was used to investigate the epitaxial phase competition between the three-layered cubic (3C) and the four-layered hexagonal (4H) perovskite polymorphs of SrMnO$_3$. Films were deposited on polycrystalline 3C-SrTiO$_3$ and 4H-SrMnO$_3$ substrates as a function of substrate orientation, temperature, and oxygen pressure. Electron backscatter diffraction data was analyzed using a dictionary-based indexing technique to determine that the eutactic orientation relationship (OR) was the preferred epitaxial orientation for both polymorphs across all conditions and substrates. An increase in substrate temperature and a decrease in oxygen pressure were found to expand the range of substrate orientations that support 3C growth from (100) to (110) and, finally, to (111) when 3C appeared as the stable phase on all SrTiO$_3$ substrate orientations. In these conditions, the metastable 4H phase was then epitaxially stabilized on nonbasal orientations of 4H-SrMnO$_3$. These results highlight how CSE can be used to understand phase competition and prepare novel metastable epitaxial films.
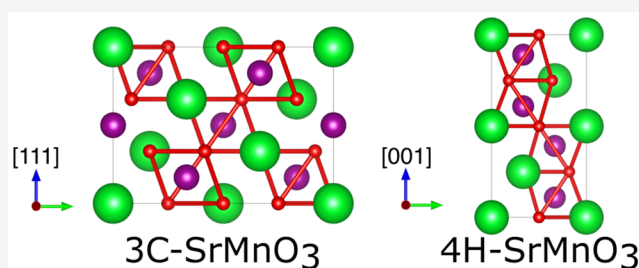
INTRODUCTION

Metastable phases are well known to form during epitaxial growth of thin films on substrates that favor thermodynamically less stable phases over more stable ones, allowing for exciting new materials to be fabricated.[1] Unfortunately, we cannot accurately predict successful synthesis pathways, including substrate structure and orientation or deposition temperature and pressure. Instead, we rely on chemical intuition based on empirical evidence conventionally obtained by low-throughput experimentation. Combinatorial substrate epitaxy (CSE) is a high-throughput epitaxial deposition technique that can accelerate our understanding of epitaxial phase competition and development of new materials; it can be used to determine phase formation and orientation relationships (ORs) between film and substrate grains over all of orientation space within a single deposition.[2−10] CSE has been used many times before to quickly reveal the epitaxial ORs of metastable phases on novel substrates and orientations.[2,3,8,10] Two of the more general conclusions from those investigations are (1) grain-over-grain epitaxy is achievable on nearly all orientations of substrates and (2) only a few low-energy ORs, such as the alignment of close-packed directions and planes, are observed across all of orientation space for large numbers of film−substrate structural pairs. Owing to the ubiquitous epitaxy and limited number of ORs, CSE can be used to map out phase competitions across synthesis space rapidly. Herein, we use CSE to continue our investigation of epitaxial phase competition between cubic and hexagonal SrMnO$_3$ as a function of substrate orientation, temperature, and oxygen

pressure, further elucidating the nature of the epitaxial phase competition that occurs during growth and demonstrating the epitaxial stabilization of metastable 4H-SrMnO$_3$.

AEMnO$_3$ (AE = Sr, Ba) materials form in many different polytypic perovskite structures that vary in the stacking of nearly close-packed (eutactic) AO$_3$ planes, leading to cubic or hexagonal stacking sequences, and in the connectivity of the BO$_6$ octahedra (corner or face sharing, depending on the stacking sequence).[11,12] Ultimately, these bonding differences impact the properties of the compound.[13,14] The thermodynamically stable structure for bulk compounds is a function of cation and oxygen compositions, the latter of which is a function of synthesis conditions. It is well known that AEMnO$_3$ materials are oxygen-deficient at high temperatures in bulk.[11,12,15,16] For SrMnO$_3$, the four-layered hexagonal (4H) phase is stable at low temperatures with oxygen contents near 3. It starts to become significantly oxygen-deficient above 1035 °C. The end member of the 4H phase is SrMnO$_{2.89}$.[12] At 1400 °C and above, the 4H phase slowly transforms into the three-layered cubic (3C) phase, lowering the oxygen content further to SrMnO$_{2.74}$.[12] Kuroda et al. determined that lowering oxygen

pressure, from atmospheric to 0.6 Pa, lowered the phase transition temperature, presumably owing to oxygen deficiency.[17] Nielsen et al. studied the role of oxygen vacancies with increasing pressure for 3C and 4H-SrMnO$_3$ and found that higher temperatures are required at higher pressures to transform 4H-SrMnO$_3$ into the 3C structure.[18] Importantly, the 3C phase can be fully reoxidized by heating in air at low temperatures.[12]

One of the challenging aspects of understanding epitaxy is that the measurement of oxygen content in films is not really possible, but trends in the bulk are often followed. In SrMnO$_3$ thin films, it has been observed that increasing the substrate temperature and lowering the deposition pressure stabilize the 3C phase.[19−21] On (111)-oriented 3C perovskite substrates, both the (111) 3C and (001) 4H phases can be epitaxial because all of these planes are the nearly close-packed (eutactic) AO$_3$ planes (each having a 6-fold planar symmetry and similar atomic arrangements). Using the idea that such substrates are close to neutral for phase selection by epitaxy, Song et al. suggested the presence of a boundary line in a pressure−temperature diagram that separates 3C and 4H stability conditions, which they correlated with the bulk transition condition.[19] The 3C phase is generally stabilized at lower oxygen pressures (around 1×10^{-6} Torr) and higher substrate temperatures (above 900 °C) due to the presence of oxygen vacancies, as in the bulk.[19] On (100)-oriented 3C perovskite substrates under typical thin film deposition conditions, it is relatively easy to stabilize 3C-SrMnO$_3$, primarily thought to originate from the preferred epitaxy of the isostructural 3C phases on the (100) 3C substrate surface. Deposition temperatures and pressures are usually above 700 °C and around 10^{-3} Torr.[21−24] On the (110) of 3C-LaAlO$_3$, Mandal et al. observed that the stable phase of SrMnO$_3$ depended on the oxygen partial pressure during deposition. The 3C phase was stabilized at a lower oxygen partial pressure compared to the 4H phase and contained mixed-valence Mn ions, whereas the 4H phase was fully oxygen stoichiometric. These studies are also consistent with bulk observations.

In this work, we report the CSE growth of SrMnO$_3$ on polycrystalline 3C-SrTiO$_3$ and 4H-SrMnO$_3$ substrates to (1) determine the effect of temperature and oxygen content on the stability of the 3C phase over all of orientation space; (2) confirm that the OR between all film−substrate pairs is the eutaxial OR; and (3) demonstrate the epitaxial stabilization of metastable 4H-SrMnO$_3$ on noneutactic orientations of 4H substrates. This work builds off a prior study, in which we deposited SrMnO$_3$ and CaMnO$_3$ using CSE in a single condition (850 °C at 2×10^{-3} Torr). In that work, 3C-SrMnO$_3$ was only stabilized on 3C substrate orientations very near to (100). On all other substrate orientations, the 4H phase was stabilized.[10] Those results indicated that the differences in interface and strain energies between the two phases were not significant to overcome the influence of the bulk volumetric formation energy of the stable 4H phase, except on the (100) substrate orientation. Because the relative energy difference is a known function of synthesis conditions, herein we present the evolution of the preferred phase of SrMnO$_3$ films on polycrystalline 3C-SrTiO$_3$ and 4H-SrMnO$_3$ substrates through the modification of substrate temperature and oxygen activity during deposition, ultimately demonstrating the epitaxial stabilization of metastable 4H-SrMnO$_3$ using polycrystalline 4H substrates prepared in-house.

■ EXPERIMENTAL DETAILS

Polycrystalline substrates were prepared using standard ceramic methods from SrTiO$_3$ powder (99%, Sigma-Aldrich) for the 3C-SrTiO$_3$ substrates and stoichiometric amounts of SrCO$_3$ (99%, Alfa Aesar) and MnO$_2$ (99.9%, Alfa Aesar) for the 4H-SrMnO$_3$ substrate. Powders were mixed in ethanol, ball-milled wet for 12 h, and dried in air at 80 °C overnight. Dried powders were ground for 10 min with a few drops of polyvinyl alcohol (PVA) and then pressed uniaxially in a stainless steel die (12 mm diameter) at pressures of >10 000 psi. Pressed pellets were placed and covered in alumina crucibles with excess powder at the bottom to reduce contamination. The 3C-SrTiO$_3$ pellet was fired in air at 700, 1000, and 1425 °C for 2, 12, and 12 h, respectively. The pressed pellet consisting of the 4H-SrMnO$_3$ precursors was reacted in air at 700 and 1000 °C for 2 and 24 h, respectively. This pellet was reground, and the 4H-SrMnO$_3$ phase was confirmed by X-ray diffraction (results not shown). The 4H-SrMnO$_3$ powder was mixed again with a few drops of PVA, pressed, and sintered in air at 700, 1000, and 1350 °C for 2, 24, and 24 h, respectively. Grain sizes were checked using a Quanta 200 scanning electron microscope (SEM) and confirmed to be larger than 10 μm, which is standard for CSE analysis.[4] The 3C-SrTiO$_3$ and 4H-SrMnO$_3$ pellets were then polished using an automatic polisher (Buehler AutoMet 250) to a mirror finish using 300, 600, and 1200 grit SiC papers, followed by 1, 0.3, and 0.05 μm alumina polishing suspensions. Pellets were thinned down to 0.5 ± 0.02 mm using a lapping fixture and an automatic polisher fitted with a 300 grit SiC paper, with the polished sides of the pellets attached to the lapping fixture's mounting block using a low-melting-temperature resin. Thinned pellets were cut into multiple smaller pieces (∼8 pieces per pellet) using a vertical diamond wire saw. Since grain sizes are larger than 10 μm, most of the substrate orientation space can be sampled in an SEM with a scan area of about 150×150 μm^2, so only one small piece was sufficient to be used as a substrate for each deposition.

A pulsed laser deposition chamber (Neocera) and KrF (λ = 248 nm) laser were used to deposit SrMnO$_3$ films. SrMnO$_3$ films were deposited using the same target as from Zhou et al.[10] 3C-SrTiO$_3$ and 4H-SrMnO$_3$ substrates were rinsed 3× in acetone and ultrasonically cleaned for 10 min, followed by the same procedure with methanol. Substrates were attached to a substrate heater using silver paste and cured at 120 °C for ∼10 min. The chamber was pumped down to background pressures of $<2 \times 10^{-5}$ Torr. The heating rate, laser density, and target-to-substrate distance were kept at 10 °C/min, 1.5 J/cm^2, and 6 cm, respectively, for all experiments.[10] Two deposition conditions were tested: (1) 900 °C at 2×10^{-3} Torr using pure O$_2$ and (2) 900 °C at 2×10^{-3} Torr using 1% O$_2$ balanced with N$_2$. Approximately 60 nm thick films were deposited for each experiment at a deposition rate of 0.1 Å/pulse, according to estimates from X-ray reflectivity (XRR) calibrations (not shown).[10] Films were cooled at a rate of 10 °C/min under 200 Torr of process gas.

Electron backscatter patterns (EBSPs) from the same area of the SrTiO$_3$ substrates and SrMnO$_3$ film surfaces were captured using electron backscatter diffraction (EBSD) in a Quanta 200 SEM using TSL EBSD Data Collection software by EDAX, as described in Zhou et al.[10] For the homoepitaxial SrMnO$_3$ film, EBSPs were collected in a Quanta 600 SEM using AZtecHKL software by Oxford Instruments. All EBSPs were indexed using dictionary-based indexing (DI), which is a process included in the open-source software package, *EMsoft*, to index EBSD patterns using a dictionary of simulated patterns.[25] Compared to the traditional Hough-based indexing implemented in commercial software, DI was able to index all patterns more consistently, even for film patterns, which are typically diffuse and noisy (most likely from internal strain and defects). Commercial software is not as robust for these types of patterns since it is based on the Hough transform, which relies on the accurate determination of Kikuchi band locations. In contrast, DI simulates the entire pattern and compares it to experimental ones using a similarity metric (the dot product of images of the patterns, parameterized as unit vectors).[25,26] This method utilizes all of the information collected
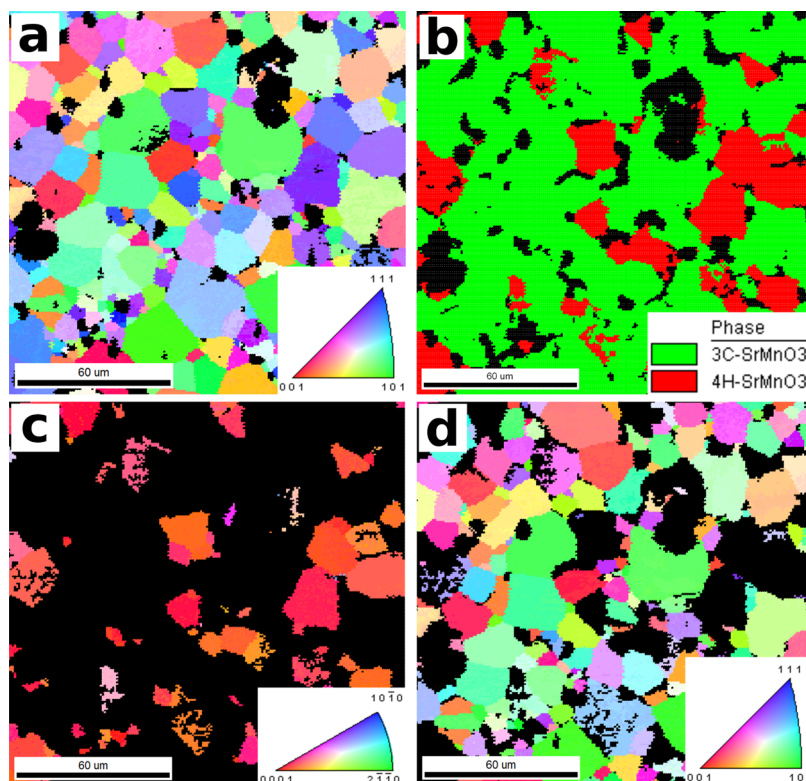
Figure 1. Orientation maps for a SrMnO₃ film deposited at 900 °C and 2 × 10⁻³ Torr O₂ on a SrTiO₃ substrate:(a) substrate, (b) film phase map, (c) 4H-SrMnO₃ film partition, and (d) 3C-SrMnO₃ film partition. The scale bar in each image is 60 μm.
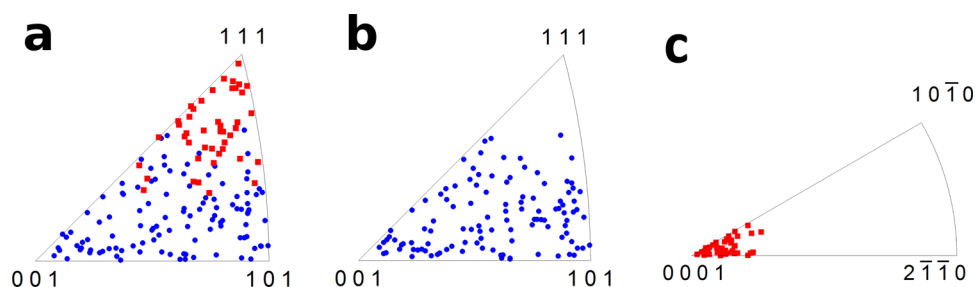
Figure 2. Mean orientations of grains from Figure 1 plotted on their respective stereographic triangles, where (a) is for the SrTiO₃ substrate, (b) is for the 3C-SrMnO₃ film, and (c) is for the 4H-SrMnO₃ film. Blue (red) dots (squares) in (a) are substrate orientations that supported 3C (4H) film growth.

from EBSPs and can handle patterns with low signal-to-noise ratios. The EBSPs from the SrMnO₃ films were indexed using 3C and 4H-SrMnO₃ master patterns with bulk lattice parameters and atomic positions. The phase of the film grains was determined using the EMdpmerge program in *EMsoft*, which compares the top dot products of each EBSP, indexed by both master patterns, and chooses the phase with the higher dot product. All of the indexing was carried out on either a computer cluster or personal computer.

DI files were converted and imported into the EDAX OIM Analysis™ software for facile mean grain orientation determination (for use in orientation relationship analysis) and construction of orientation maps. All raw orientation maps were processed using a minimum grain size of 5 μm and a grain tolerance angle of 5°. Holes or poorly indexed points were removed by setting limits on the image quality and/or confidence interval. Mean orientations of the selected corresponding substrate and film grains were recorded for OR analysis, which utilizes an in-house python program that calculates the minimum angle between reference directions in the substrate and film.[3]

■ RESULTS

Figure 1a shows the orientation map of a SrTiO₃ substrate; each grain is colored with respect to the mean orientation within the grain. Figure 1b−d represents phase and orientation maps of the same area after deposition of an ≈60 nm SrMnO₃ film. The shapes of the film grains are similar to those in the substrate, indicating that growth is grain-over-grain, regardless of orientation or phase. The phase map in Figure 1b is colored according to the phase of the film as determined by DI, where green areas are grains indexed as 3C-SrMnO₃ and red areas are grains indexed as 4H-SrMnO₃ (black areas as holes or low-quality areas). The dominant phase of the SrMnO₃ film is indexed as 3C-SrMnO₃, and the minority phase is indexed as 4H-SrMnO₃. This is in contrast to the SrMnO₃ films deposited at 850 °C and 2 mTorr O₂,[10] which had very few 3C-SrMnO₃ grains. Thus, increasing the substrate temperature by ≈50 °C significantly increases the number of SrTiO₃ substrate grains that support 3C growth.
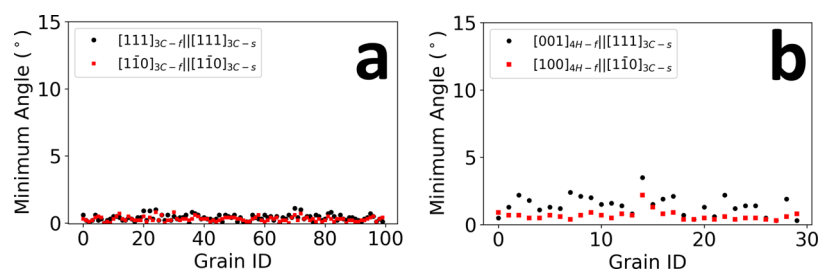
Figure 3. Plot of grain ID versus minimum angle between eutactic planes and directions for the SrMnO$_3$ film deposited on SrTiO$_3$ at 900 °C and 2 × 10^{-3} Torr O$_2$, where (a) plots the ORs for the 3C film and substrate and (b) plots the ORs for the 4H film and substrate. Black (red) dots are the angular deviations from the eutactic planes (directions).
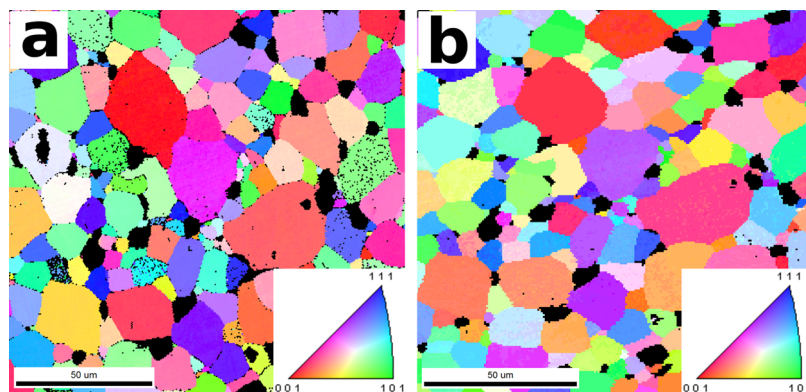
Figure 4. Orientation maps for a SrMnO$_3$ film deposited at 900 °C and 2 × 10^{-3} Torr using 1% O$_2$ on a SrTiO$_3$ substrate, where (a) is the substrate and (b) is the 3C-SrMnO$_3$ film. The scale bar in each image is 50 μm.
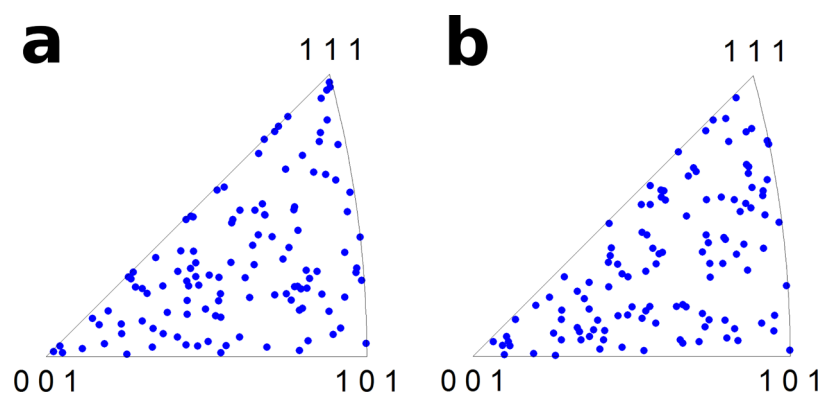
Figure 5. Mean orientations of grains from Figure 4 plotted on their respective stereographic triangles, where (a) is for the substrate and (b) is for the 3C-SrMnO$_3$ film. Blue dots in (a) are substrate orientations that supported 3C film growth.

Figure 1c,d shows the orientation maps of the 3C-SrMnO$_3$ and 4H-SrMnO$_3$ film partitions, respectively. The orientations (reddish colors) of the 4H-SrMnO$_3$ film grains are clustered near (001) in Figure 1c, and the corresponding substrate grain orientations (bluish colors) are near the (111). The orientations of the 3C-SrMnO$_3$ vary across the color spectrum, except for the absence of dark blue (near (111)) and are colored similarly to their corresponding substrate grains, indicating that they are oriented similarly in the z-direction (normal to the surface). A few film grains are indexed as both 3C and 4H, similar to those reported previously.[10]

Mean grain orientations of the SrTiO$_3$ substrate and SrMnO$_3$ film are plotted on their respective stereographic triangles in Figure 2. Blue dots represent orientations of the substrate (Figure 2a) that supported 3C film orientations (Figure 2b). Red squares in Figure 2a represent orientations of

the substrate grains that supported 4H film orientations (Figure 2c). Substrate orientations are spread uniformly throughout the orientation space, indicating that this area is representative of the entire substrate surface. The substrate grains that supported 4H film growth have orientations near the (111), with an angular spread of up to 24°. For the 4H film in Figure 2c, the grain orientations are located near (001), with a spread of up to 33° away from (001). Substrate grains that supported 3C growth are generally spread throughout the rest of orientation space. Corresponding 3C-SrMnO$_3$ film–grain orientations in Figure 2b are spread similarly throughout the cubic orientation space, except for orientations less than 13° from the (111). These observations are reasonable if the films have the eutactic OR, regardless of the phase.[10]

Orientation relationships (ORs) were determined using an in-house Python program, which calculates the minimum angle

between a reference direction in the substrate and a reference direction in the film. The directions for all ORs presented herein correspond to the eutactic planes and directions for 4H and 3C structures. In Figure 3a, the minimum angles between the 3C-SrMnO$_3$ film grains and SrTiO$_3$ substrate are plotted for each grain. Black dots correspond to angles between eutactic planes, and red dots correspond to those between eutactic directions. The average angle between eutactic planes (directions) for 100 3C film–grain pairs is 0.39° (0.29°) ± 0.23° (0.17°). For the data presented in Figure 3b, the minimum average angle for eutactic planes (directions) between 30 4H film–grain pairs is 1.34° (0.62°) ± 0.63° (0.22°). The primary OR for the 3C and 4H-SrMnO$_3$ films on SrTiO$_3$ is the one that aligns the eutactic planes and directions, as seen in Zhou et al.[10]

The deposition of a SrMnO$_3$ film on a polycrystalline 3C-SrTiO$_3$ substrate was repeated using a 1% O$_2$ process gas. The deposition temperature was 900 °C, and the total deposition pressure remained at 2×10^{-3} Torr, resulting in an effective oxygen partial pressure of around 2×10^{-5} Torr O$_2$ (the exact partial pressure not measured). EBSD data was processed using DI, and orientation maps were constructed using OIM (maps are shown in Figure 4). A phase map is not shown for this deposition because all film grains were indexed as 3C-SrMnO$_3$. Grain shapes between the substrate and film in Figure 4a,b, respectively, appear to be distorted due to slight sample tilting in the SEM chamber and charging effects, but they still retain similar enough shapes for comparison to conclude that grain-over-grain growth dominates.

Mean orientations of the SrTiO$_3$ and 3C-SrMnO$_3$ films are shown in Figure 5. Blue dots in Figure 5a represent SrTiO$_3$ substrate orientations that supported 3C growth. Substrate orientations are spread throughout orientation space, indicating that the scanned surface is representative of the whole substrate. Similar observations are seen for the mean orientations of 3C-SrMnO$_3$ film grains in Figure 5b.

Orientation analysis of the minimum angle between eutactic planes and directions of the 3C-SrMnO$_3$ film and SrTiO$_3$ substrate is plotted for 109 film–substrate grains in Figure 6.
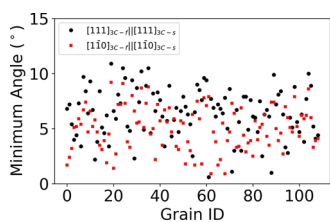
Figure 6. Plot of grain ID and angular deviation from the eutactic angle and direction for the film grains from Figure 4. Black (red) dots are the angles for eutactic planes (directions).

The average angle between eutactic planes (directions) is 6.38° (5.01°) ± 2.25° (1.95°). The angles have larger average values and standard deviations compared to those in Figure 3, the origin for which is unclear. However, lower oxygen contents in the film during growth may lead to structural distortions from cubic symmetry that decreases the quality of the alignment of eutactic directions and planes.[27] Nevertheless, the values are taken as an indication that the eutactic OR remains the preferred OR between the 3C substrate and 3C film. Finally, if we assume that the (111) orientation is neutral with respect to epitaxial stabilization, these observations argue that the 3C

phase is more stable than the 4H phase in these deposition conditions.

Using the same deposition conditions under which 3C-SrMnO$_3$ was stabilized over all orientations of SrTiO$_3$, a SrMnO$_3$ film was deposited on a 4H-SrMnO$_3$ polycrystalline substrate. The red box in Figure 7a outlines the same area of the substrate surface as that of the film in Figure 7b–d. The film maps are elongated due to charging in the SEM chamber. As a consequence, the 25 μm scale bar is not accurate in the vertical direction of the film maps. This, however, did not affect identification of corresponding film grains to substrate grains since the general shape of grains was retained. The spread of 4H-SrMnO$_3$ substrate orientations in Figure 7a well captures the whole orientation range, making this area suitable for CSE. The film phase map, 4H-SrMnO$_3$ map, and 3C-SrMnO$_3$ map are shown in Figure 7b–d, respectively. Under these deposition conditions, a majority of the film was indexed as 4H-SrMnO$_3$. In Figure 7c, the 4H-SrMnO$_3$ partition is colored mostly blue-green, indicating that the 4H phase tended to grow on nonbasal orientations, with a few exceptions. In Figure 7d, the 3C-SrMnO$_3$ grains do not appear to favor one orientation over another.

The mean grain orientations of the 4H-SrMnO$_3$ substrate and their corresponding film grains are plotted in Figure 8. 4H-SrMnO$_3$ substrate grains near the (001) primarily favor 3C growth, as indicated by the blue dots in Figure 7a. Though bunched toward (001), these substrate grains are spread out over 67° of orientation space. The corresponding 3C film–grain orientations in Figure 7c are distributed throughout the cubic orientation space, which covers 17° away from the (111), with the exception of two grains. Nonbasal oriented 4H substrate grains supported similarly oriented 4H film grains. While grains more than 16° away from the (001) supported only 4H growth, films spread over the range of 16–67° away from the (001) supported the growth of both phases. Assuming that the eutactic (001) plane is relatively neutral toward film growth, as is the (111) of 3C-SrTiO$_3$, this observation agrees that the 3C phase is thermodynamically preferred in these lower-oxygen-pressure growth conditions. Thus, the 4H grains observed in this deposition indicate epitaxial stabilization of this polymorph, made possible by using in-house-prepared substrate exposing nonbasal orientations.

Using the mean grain orientations of the 4H-SrMnO$_3$ substrate grains and corresponding film grains, the minimum angles between eutactic planes and directions were calculated and plotted in Figure 9. The average angle between eutactic planes (directions) for the 49 3C film grains in Figure 9a is 2.5° (2.8°) ± 1.2° (1.1°). For the 127 4H film grains in Figure 9b, the average angle between eutactic planes (directions) is 3.7° (2.4°) ± 1.0° (1.1°). These observations again indicate that the eutactic OR is preferred in these conditions, as expected.

■ DISCUSSION

CSE was used to investigate the orientation relationships and phase stability of SrMnO$_3$ films deposited on 3C-SrTiO$_3$ and 4H-SrMnO$_3$ polycrystalline substrates, and several elegant outcomes are found using the high-throughput epitaxy method. First, films adhere to a single general orientation relationship (OR) known as the eutactic OR, regardless of the orientation of the substrate or the film–substrate phase-pair considered, reinforcing its generality in describing epitaxy.
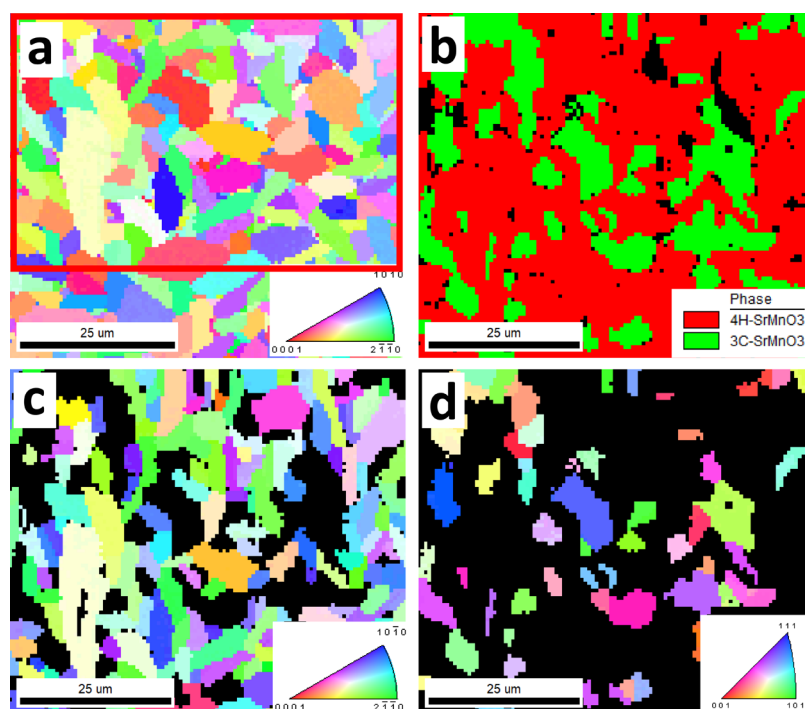
Figure 7. Orientation maps for a SrMnO$_3$ film deposited at 900 °C and 2 × 10^{-5} Torr O$_2$ on a 4H-SrMnO$_3$ substrate: (a) substrate, (b) film phase map, (c) 4H-SrMnO$_3$ film partition, and (d) 3C-SrMnO$_3$ film partition.
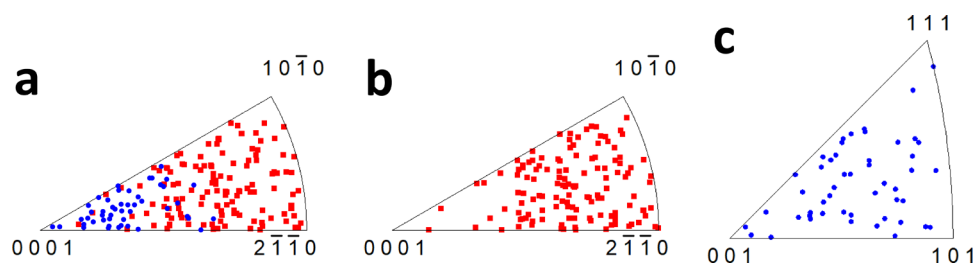
Figure 8. Mean orientations of grains from Figure 7 plotted on their respective stereographic triangles, where (a) is for the 4H-SrMnO$_3$ substrate, (b) is for the 4H-SrMnO$_3$ film, and (c) is for the 3C-SrMnO$_3$ film. Blue (red) dots (squares) in (a) are substrate orientations that supported 3C (4H) film growth.
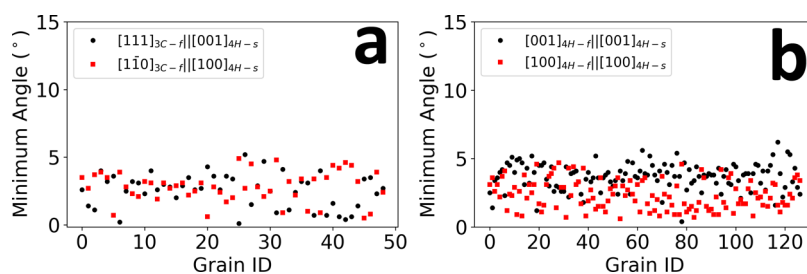
Figure 9. Plot of grain ID versus minimum angle between eutactic planes and directions for the homoepitaxial SrMnO$_3$ film deposited at 900 °C and 2 × 10^{-5} Torr O$_2$, where (a) plots the ORs for the 3C film and substrate and (b) plots the ORs for the 4H film and substrate. Black (red) dots are the angular deviations from the eutactic planes (directions).

Second, both the 3C and 4H polymorphs were shown to be both chemically and epitaxially stabilized, with phase stability being a function of deposition conditions, as well as substrate orientation and structure. Films were deposited at 900 °C (higher than temperatures than previously reported[10]) and in two different oxygen pressures—conditions were targeted to increase the relative chemical stability of 3C-SrMnO$_3$ with respect to 4H-SrMnO$_3$. Indeed, in the lower-oxygen-pressure condition, 3C-SrMnO$_3$ appears to be the more stable phase,

which allows for the epitaxial stabilization of the 4H phase on a 4H substrate but only for nonbasal orientations. In this section, we discuss these observations more broadly.

Orientation Relationship. The preferred epitaxial orientation relationship between all films and substrates presented herein is the eutactic one, which aligns the eutactic (nearly close-packed) planes and directions. These results agree with our previous study of similar materials, for both 3C-CaMnO$_3$ on 4H-SrMnO$_3$ and 4H-SrMnO$_3$ on 3C-SrTiO$_3$, deposited at

850 °C.[10] Furthermore, for many other film−substrate pairs that are readily described as eutactic structures, the eutactic orientation relationship is overwhelmingly the main epitaxial OR, with angular deviations less than 5°.[2−10,28] The prevalence of the eutactic relationship over all other ORs suggests that the alignment of eutactic planes and directions is strongly energetically preferred. This is reinforced here, even with significant changes in oxygen content and deposition conditions. While the average and standard deviation values for the angles between the eutactic directions (planes) are relatively large (6.38° (5.01°) ± 2.25° (1.95°)) for the 3C-SrMnO$_3$ film deposited on SrTiO$_3$ in low oxygen pressures (where 3C is the stable phase), the eutactic OR is still the simplest descriptor of epitaxy. The relatively large values likely arise from relaxations on reoxygenation during cooling or from noncubic symmetries for oxygen-deficient SrMnO$_{3−x}$ that cause deviations from the average cubic eutaxy.[27,29,30] Further investigations are needed to understand these values. Ultimately, having a singular OR define the preferred epitaxy means that only a small number of competitive events describe epitaxy generally and that only very few computations would be needed to quantify this competition.[31]

Chemical versus Epitaxial Stability. Stabilization of the different SrMnO$_3$ phases is achieved through two means in this paper: chemical and epitaxial. Chemical stability can be described as the phase with the lower free energy in the given thermodynamic conditions including temperature, oxygen pressure, and stoichiometry.[32] Epitaxial stability can be described as a chemically metastable polymorph that is stabilized by interactions with the substrate during crystallization events, usually when interfacial and strain energy terms are comparable to the volumetric bulk terms for small epitaxial nuclei.[1] The difference between the two types of stabilities can be readily explored using CSE and is easily explained using preferences on the low Miller index substrate surfaces.

Because the only observed OR is the eutactic OR, we can consider the eutactic planes—(111) of 3C-SrMnO$_3$ and the (001) of 4H-SrMnO$_3$—as the most energetically neutral surfaces. Both polymorphs are likely to form coherent interfaces of relatively low energy and therefore have relatively small epitaxial energy differences.[33] This agrees with Song's assertions for SrMnO$_3$.[19] As such, the phases that form on these surfaces are good indicators of chemical stability. In the high-oxygen-pressure deposition condition, the 4H-SrMnO$_3$ phase is observed to grow on all surfaces near the (111) of 3C-SrTiO$_3$. Similar observations were made at lower temperatures.[10,19] This indicates that the 4H phase is chemically stable. In the low-oxygen-pressure deposition condition, the 3C-SrMnO$_3$ phase is observed to grow on all surfaces, including near the (111) of 3C-SrTiO$_3$, as well as near the (001) of 4H-SrMnO$_3$. These observations indicate that the 3C phase is chemically stable in these conditions. In general, these results agree with observations made by Song et al.[19] on single crystals of SrTiO$_3$, as well as with the general understanding of phase stability in SrMnO$_3$.[17,21] Once chemical stability is established, any other phase observed must be through epitaxial stability.

3C Epitaxial Stabilization. Both the (100) and (110) surfaces of the 3C-SrTiO$_3$ substrate have symmetries with which only the 3C phase is coherent (the 4H can be epitaxial but has incoherent interfaces) and both should support epitaxial stabilization. At 850 °C in pure oxygen environments,[10] however, only surfaces very near the (100) epitaxially

stabilized the 3C polymorph. Additionally, not all (100) substrates were completely 3C (some areas indexed as 4H, confirmed by both OIM software and DI).[10] For films deposited at 900 °C (in otherwise identical conditions), we see an expansion of the orientations of SrTiO$_3$ that support epitaxially stabilized 3C-SrMnO$_3$ including both the (100) and (110) SrTiO$_3$ surfaces, as well as most surfaces rotated away from these corners of the stereographic triangle. This increase in orientations that lead to epitaxial stabilization supports the hypothesis that the energetic difference between phases decreases with the increasing temperature. Combined, these results suggest that the penalties of higher interface energy and/or strain energy between polytypes are not significant enough to overcome the volumetric formation energy of the stable 4H phase at 850 °C[10] but can at 900 °C. Thus, temperature plays a significant role in the epitaxial stabilization of 3C-SrMnO$_3$. These findings also suggest that the different low-index surfaces have different capabilities for overcoming chemical metastability, with (100) being better than (110) and the (111) being relatively neutral.

4H Epitaxial Stabilization. Low-index surfaces of 4H-SrMnO$_3$ rotated away from the eutactic (001) surface are expected to have symmetries with which only the 4H phase is coherent (the 3C can be epitaxial but has incoherent interfaces) and thus should support 4H epitaxial stabilization. The only orientation of a hexagonal crystal available commercially is the (001) of Al$_2$O$_3$ and 4H-SiC, an orientation that is neutral for epitaxial stabilization. Here, we investigated 4H epitaxial stabilization using CSE and substrates prepared from readily sintered 4H-SrMnO$_3$ pellets. In the low-oxygen-pressure-deposition conditions at 900 °C, where 3C is chemically stable, 3C forms epitaxially on (001) surfaces (or (0001) in the Miller−Bravais notation used in Figure 8). As expected, on substrate surfaces rotated significantly away (by more than 67°) from the (001), only 4H-SrMnO$_3$ films formed on 4H-SrMnO$_3$. This is also an indication that these surfaces are stable with respect to decomposition of the 3C phase during the deposition. Very near to the (001) of the 4H substrate, only the 3C phase formed, also as expected (though in this experiment, only two grains were characterized). In the angular range of 16−67° of the 4H substrate (see Figure 8a), both phases were observed to form. Keep in mind that the angular range of the 3C fundamental zone is 35−55° away from the (111), while it is 90° for the 4H fundamental zone (rotated away from the (001)). In fact, 3C grains formed with orientations spanning across the entire 3C fundamental zone, as seen in Figure 8c. In spite of this mixed-phase formation, the prevalence of 3C film grains is higher within the first 43° away from the 4H substrate (001) grains and lower within the next 24°, until it is absent in the last 23°.

This significant overlap in phase stability with respect to orientation may reflect several factors. First, the difference in energy between the chemical stability of the two phases may be relatively small, and therefore the probability of either phase formation may be close on many orientations.[34] Second, the nature of the surfaces is unknown for these crystals, especially for high-index orientations (those rotated away from the corners of the stereographic projection). The Wulff shape of 4H-SrMnO$_3$ is also unknown, but hexagonal basal planes and eutactic planes often play important roles in the Wulff shape and in the terrace−ledge−kink (TLK) model of the surface structure.[35] Assuming this is the case, the (001) may be the stable surface and/or simply dominate a TLK structure of the

surface over a wide range of orientation space near the (001). Third, high-index surfaces near the (001) may be less stable toward decomposition to the 3C phase, which is chemically stable in these thermodynamic conditions. If so, such surfaces may themselves have transformed and then support 3C growth. This would require the transformed surface to retain the same epitaxial (eutactic) relationships with the original substrate structure. Fourth, the 3C phase may have some small kinetic advantage, having a smaller unit cell and smaller repeat period perpendicular to the eutactic planes, which gives it a small advantage in a flat energy landscape. It should be pointed out that both polymorphs form readily in the different conditions,[12,17,19] so any kinetic preference should be slight, if at all. Also, because we used mixed gases at the same overall pressures, there were only nominal differences in the growth rates and expected kinetics between the two deposition conditions used. While all of these possibilities are interesting, none of them were investigated further, as 4H epitaxial stabilization is readily demonstrated for all orientations greater than 67° away from the (001). Presumably, higher temperatures and lower oxygen pressures would further decrease the range of 4H stability on these 4H substrates.

Substrate Preparation. Because of the significant difference in the 3C-$SrMnO_3$ phase stability with temperature, substrate preparation should be discussed. In the present work, 3C-$SrTiO_3$ and 4H-$SrMnO_3$ polycrystalline substrates were meticulously thinned to thicknesses of 0.5 ± 0.02 mm using a lapping fixture, similar to the thickness of typical single crystals. For the polycrystalline substrates used in Zhou et al.,[10] substrates were not thinned to 0.5 mm using the lapping fixture; they were up to 1 mm thick and did not necessarily have perfectly parallel surfaces. Therefore, it is possible that the substrate surface temperature from Zhou et al. was more than 50 °C cooler than the difference in the heater temperatures. Thinner substrates should also diminish any difference between the chemically different $SrTiO_3$ and $SrMnO_3$ substrates. Since the substrates used herein are similar to typical single crystals, we expect our results to be comparable to single-crystal work.[19,21,23]

In general, for CSE, it is imperative to carefully control the quality and thickness of polycrystalline substrates so that results can be compared to single-crystal work and repeated. As mentioned above, the thickness of substrates should be carefully controlled so that the temperature on the surface during growth is comparable in between depositions and substrates. The density of sintered substrates should also be considered—ideally, they should be above 92% of the theoretical density so that the effect of pores in the substrate does not significantly vary the temperature across the substrate surface. Polishing the sintered substrate can also be a factor in variations between CSE experiments as surface damage from polishing can affect the growth and quality of the film. Since the majority phase of these $SrMnO_3$ films is sensitive to temperature and oxygen partial pressure, it is expected that the results presented in this paper can be repeated but with some slight variation in the phase fraction and/or in the minimum angles between eutactic planes/directions due to variations in substrate preparation. For example, for a $SrMnO_3$ film deposited on polycrystalline $SrTiO_3$ at 850 °C under 2 mTorr O_2 (repeated conditions from Zhou et al.[10] on a substrate thinned to 0.5 mm as described herein; results not shown), it was found that some (110) $SrTiO_3$ supported 3C-$SrMnO_3$, indicating that substrate thickness most likely played

a large role on the surface temperature during deposition. Finally, it is important to note that should substrate quality differ between depositions, the OR is still expected to be the eutactic one, as well as the trend that increasing temperature/decreasing oxygen partial pressure stabilizes the 3C phase.

CONCLUSIONS

The temperature, pressure, and orientation dependence of the phase competition between 3C and 4H-$SrMnO_3$ films on $SrTiO_3$ and 4H-$SrMnO_3$ polycrystalline substrates were investigated using CSE. DI is used exclusively for orientation and phase determination because of its ability to index thin film patterns better than commercially available Hough-based indexing software. This method paves the way for EBSD to be used more frequently and reliably in thin film studies, especially for CSE experiments, where traditional thin film analysis methods such as XRD and transmission electron microscopy cannot be used easily. From the indexed orientation data, the ORs determined for all films and substrates in this paper agree with the previous finding that the eutactic OR aligns the eutactic planes and directions for all polymorphs of $SrMnO_3$ on $SrTiO_3$ and 4H-$SrMnO_3$, regardless of deposition conditions. Additionally, the eutactic planes were found to be good indicators of the chemically stable phase, and any other phase observed must be through epitaxial stability. This is true regardless of the substrate structure. The results further support the same idea from Zhou et al.[10] in that CSE can quickly demonstrate the nature of epitaxial stabilization of competing polymorphs and that the conclusions drawn from experimental work may allow computational predictions to be carried out for the energetic competition between polymorphs of similar thin film materials on substrates.

AUTHOR INFORMATION

Corresponding Author

Paul A. Salvador − *Department of Materials Science and Engineering, Carnegie Mellon University, Pittsburgh, Pennsylvania 15213, United States*; Email: paulsalvador@cmu.edu

Authors

Catherine Zhou − *Department of Materials Science and Engineering, Carnegie Mellon University, Pittsburgh, Pennsylvania 15213, United States*; orcid.org/0000-0003-3387-7979

Gregory S. Rohrer − *Department of Materials Science and Engineering, Carnegie Mellon University, Pittsburgh, Pennsylvania 15213, United States*; orcid.org/0000-0002-9671-3034

Marc De Graef − *Department of Materials Science and Engineering, Carnegie Mellon University, Pittsburgh, Pennsylvania 15213, United States*

Complete contact information is available at:
https://pubs.acs.org/10.1021/acs.cgd.1c00429

Notes

The authors declare no competing financial interest.

ACKNOWLEDGMENTS

■ REFERENCES

(1) Gorbenko, O. Y.; Samoilenkov, S. V.; Graboy, I. E.; Kaul, A. R. Epitaxial stabilization of oxides in thin films. *Chem. Mater.* **2002**, *14*, 4026−4043.

(2) Burbure, N. V.; Salvador, P. A.; Rohrer, G. S. Orientation and Phase Relationships between Titania Films and Polycrystalline BaTiO₃ Substrates as Determined by Electron Backscatter Diffraction Mapping. *J. Am. Ceram. Soc.* **2010**, *93*, 2530−2533.

(3) Zhang, Y.; Schultz, A. M.; Li, L.; Chien, H.; Salvador, P. A.; Rohrer, G. S. Combinatorial Substrate Epitaxy: A High-Throughput Method for Determining Phase and Orientation Relationships and Its Application to BiFeO₃/TiO₂ Heterostructures. *Acta Mater.* **2012**, *60*, 6486−6493.

(4) Havelia, S.; Wang, S.; Balasubramaniam, K. R.; Schultz, A. M.; Rohrer, G. S.; Salvador, P. A. Combinatorial Substrate Epitaxy: A New Approach to Growth of Complex Metastable Compounds. *CrystEngComm* **2013**, *15*, 5434−5441.

(5) Schultz, A. M.; Zhu, Y.; Bojarski, S. A.; Rohrer, G. S.; Salvador, P. A. Eutaxial Growth of Hematite Fe₂O₃ Films on Perovskite SrTiO₃ Polycrystalline Substrates. *Thin Solid Films* **2013**, *548*, 220−224.

(6) Pravarthana, D.; Lebedev, O. I.; David, A.; Fouchet, A.; Trassin, M.; Rohrer, G. S.; Salvador, P. A.; Prellier, W. Metastable monoclinic [110] layered perovskite Dy₂Ti₂O₇ thin films for ferroelectric applications. *RSC Adv.* **2019**, *9*, 19895−19904.

(7) Lacotte, M.; David, A.; Pravarthana, D.; Grygiel, C.; Rohrer, G. S.; Salvador, P. A.; Velazquez, M.; de Kloe, R.; Prellier, W. Growth of Ca₂MnO₄ Ruddlesden-Popper structured thin films using combinatorial substrate epitaxy. *J. Appl. Phys.* **2014**, *116*, No. 245303.

(8) Wittkamper, J.; Xu, Z.; Kombaiah, B.; Ram, F.; De Graef, M.; Kitchin, J. R.; Rohrer, G. S.; Salvador, P. A. Competitive Growth of Scrutinyite (α-PbO₂) and Rutile Polymorphs of SnO₂ on All Orientations of Columbite CoNb₂O₆ Substrates. *Cryst. Growth Des.* **2017**, *17*, 3929−3939.

(9) Santosh, M.; Lacotte, M.; David, A.; Boullay, P.; Grygiel, C.; Pravarthana, D.; Rohrer, G. S.; Salvador, P. A.; Padhan, P.; Lüders, U.; Wang, J.; Prellier, W. Pulsed Laser Deposition of Sr₂FeMoO₆ Thin Films Grown on Spark Plasma Sintered Sr₂MgWO₆ Substrates. *J. Phys. D: Appl. Phys.* **2017**, *50*, No. 235301.

(10) Zhou, C.; De Graef, M.; Dabrowski, B.; Rohrer, G. S.; Salvador, P. A. Combinatorial substrate epitaxy investigation of polytypic growth of AEMnO₃ (AE=Ca, Sr). *J. Am. Ceram. Soc.* **2020**, *103*, 2225−2234.

(11) Negas, T.; Roth, R. S. Phase Equilibria and Structural Relations in the System BaMnO₃₋ₓ. *J. Solid State Chem.* **1971**, *3*, 323−339.

(12) Negas, T.; Roth, R. S. The System SrMnO₃₋ₓ. *J. Solid State Chem.* **1970**, *1*, 409−418.

(13) Søndenå, R.; Ravindran, P.; Stolen, S.; Grande, T.; Hanfland, M. Electronic Structure and Magnetic Properties of Cubic and Hexagonal SrMnO₃. *Phys. Rev. B* **2006**, *74*, No. 144102.

(14) Søndenå, R.; Stolen, S.; Ravindran, P.; Grande, T.; Allan, N. L. Corner- versus Face-Sharing Octahedra in AMnO₃ Perovskites (A=Ca, Sr, and Ba). *Phys. Rev. B* **2007**, *75*, No. 184105.

(15) Caignaert, V.; Nguyen, N.; Hervieu, M.; Raveau, B. Sr₂Mn₂O₅, an oxygen-defect perovskite with Mn(III) in square pyramidal coordination. *Mater. Res. Bull.* **1985**, *20*, 479−484.

(16) Taguchi, H.; Nagao, M.; Sato, T.; Shimada, M. High-Temperature Phase Transition of CaMnO₃₋δ. *J. Solid State Chem.* **1989**, *78*, 312−315.

(17) Kuroda, K.; Shinozaki, K.; Uematsu, K.; Mizutani, N.; Kato, M. Oxygen-Deficiency-Induced Polymorphs and Electrical Conductivity of SrMnO₃₋ₓ. *J. Am. Ceram. Soc.* **1980**, *63*, 109−110.

(18) Nielsen, M. B.; Ceresoli, D.; Parisiades, P.; Prakapenka, V. B.; Yu, T.; Wang, Y.; Bremholm, M. Phase Stability of the SrMnO₃ Hexagonal Perovskite System at High Pressure and Temperature. *Phys. Rev. B* **2014**, *90*, No. 214101.

(19) Song, R.-N.; Hu, M.-H.; Chen, X.-R.; Guo, J.-D. Epitaxial Growth and Thermostability of Cubic and Hexagonal SrMnO₃ Films on SrTiO₃(111). *Front. Phys.* **2015**, *10*, 321−326.

(20) Langenberg, E.; Guzmán, R.; Maurel, L.; de Baños, L. M.; Morellón, L.; Ibarra, M. R.; Herrero-Martín, J.; Blasco, J.; Magén, C.; Algarabel, P. A.; Pardo, J. A. Epitaxial Stabilization of the Perovskite Phase in (Sr₁₋ₓBaₓ)MnO₃ Thin Films. *ACS Appl. Mater. Interfaces* **2015**, *7*, 23967−23977.

(21) Mandal, A. K.; Rawat, R.; Sah, R. K.; Wadikar, A.; Choudhary, R. J.; Phase, D. M. Magnetic and electronic properties of off-stoichiometric SrMnO₃ thin film on SrTiO₃ (100) substrate. *AIP Conf. Proc.* **2019**, *2115*, No. 030321.

(22) Maurel, L.; Marcano, N.; Prokscha, T.; Langenberg, E.; Blasco, J.; Guzmán, R.; Suter, A.; Magén, C.; Morellón, L.; Ibarra, M. R.; Pardo, J. A.; Algarabel, P. A. Nature of Antiferromagnetic Order in Epitaxially Strained Multiferroic SrMnO₃ Thin Films. *Phys. Rev. B* **2015**, *92*, No. 024419.

(23) Kobayashi, S.; Tokuda, Y.; Ohnishi, T.; Mizoguchi, T.; Shibata, N.; Sato, Y.; Ikuhara, Y.; Yamamoto, T. Cation Off-Stoichiometric SrMnO₃₋δ Thin Film Grown by Pulsed Laser Deposition. *J. Mater. Sci.* **2011**, *46*, 4354−4360.

(24) Francis, A. J.; Salvador, P. A. Synthesis, structures, and physical properties of yttrium-doped strontium manganese oxide films. *Mater. Res. Soc. Symp. Proc.* **2002**, *718*, No. 94.

(25) Jackson, M. A.; Pascal, E.; De Graef, M. Dictionary Indexing of Electron Back-Scatter Diffraction Patterns: a Hands-On Tutorial. *Integr. Mater. Manuf. Innovation* **2019**, *8*, 226−246.

(26) Graef, M. D.; Jackson, M.; Kleingers, J.; Zhu, C.; Atkinson, M.; Wright, S.; Ånes, H. *EMsoft-org/EMsoft: EMsoft Release 5.0.0*, 2019.

(27) Agrawal, P.; Guo, J.; Yu, P.; Hébert, C.; Passerone, D.; Erni, R.; Rossell, M. D. Strain-driven oxygen deficiency in multiferroic SrMnO₃ thin films. *Phys. Rev. B* **2016**, *94*, No. 104101.

(28) Wong, F. J.; Ramanathan, S. Nonisostructural complex oxide heteroepitaxy. *J. Vac. Sci. Technol. A* **2014**, *32*, No. 040801.

(29) Lee, J. H.; Rabe, K. M. Epitaxial-strain-induced multiferroicity in SrMnO₃ from first principles. *Phys. Rev. Lett.* **2010**, *104*, No. 207204.

(30) Daoud-Aladine, A.; Martin, C.; Chapon, L. C.; Hervieu, M.; Knight, K. S.; Brunelli, M.; Radaelli, P. G. Structural phase transition and magnetism in hexagonal SrMnO₃ by magnetization measurements and by electron, x-ray, and neutron diffraction studies. *Phys. Rev. B* **2007**, *75*, No. 104417.

(31) Xu, Z.; Salvador, P.; Kitchin, J. R. First-Principles Investigation of the Epitaxial Stabilization of Oxide Polymorphs: TiO₂ on (Sr,Ba)TiO₃. *ACS Appl. Mater. Interfaces* **2017**, *9*, 4106−4118.

(32) Dabrowski, B.; Chmaissem, O.; Mais, J.; Kolesnik, S.; Jorgensen, J. D.; Short, S. Tolerance factor rules for Sr₁₋ₓ₋ᵧCaₓBaᵧMnO₃ perovskites. *J. Solid State Chem.* **2003**, *170*, 154−164.

(33) Sutton, A. P. Interfaces in Crystalline Materials. In *Monographs on the Physics and Chemistry of Materials*; Clarendon: Oxford, 1995; p 51.

(34) Davis, H.; Evans, D. Statistical Mechanics of Phases, Interfaces, and Thin Films. In *Advances in Interfacial Engineering Series*; VCH, 1996.

(35) Einstein, T. *Handbook of Crystal Growth*, 2nd ed.; Elsevier Inc., 2015; Vol. *1*, pp 215−264.